Draft version March 17, 2024
Typeset using LaTeX **twocolumn** style in AASTeX63

arXiv:2008.05097v3 [astro-ph.HE] 19 Oct 2020

Magnetar giant flare origin for GRB 200415A inferred from a new scaling relation and its implications

Hai-Ming Zhang,[1,2] Ruo-Yu Liu,[1,2] Shu-Qing Zhong,[1,2] and Xiang-Yu Wang[1,2]

[1]*School of Astronomy and Space Science, Nanjing University, Nanjing 210023, China; xywang@nju.edu.cn; ryliu@nju.edu.cn*
[2]*Key laboratory of Modern Astronomy and Astrophysics (Nanjing University), Ministry of Education, Nanjing 210023, China*

ABSTRACT

Soft gamma-ray repeaters (SGRs) are mainly a Galactic population and originate from neutron stars with intense ($B \simeq 10^{15}$ G) magnetic fields ('magnetars'). Occasionally, a giant flare occurs with enormous intensity, displaying a short hard spike, followed by a weaker, oscillatory phase which exhibits the rotational period of the neutron star. If the magnetar giant flares occur in nearby galaxies, they would appear as cosmic short-hard gamma-ray bursts (GRBs) without detecting the weak oscillatory phase. Recently, a short-hard GRB named GRB 200415A was detected, with a position coincident with the Sculptor Galaxy (NGC 253), rasing the question whether it is a classic short GRB or a magentar giant flare. Here we show that magnetar giant flares follow a scaling relation between the spectral peak energy and the isotropic energy in $1\,\mathrm{keV} - 10\,\mathrm{MeV}$, i.e., $E_\mathrm{p} \propto E_\mathrm{iso}^{1/4}$, and locate in a distinct region of the $E_\mathrm{p} - E_\mathrm{iso}$ plane from that of classic short GRBs. The relation can be well understood in the model that giant flares arise from the photosphere emissions of relativistically expanding fireball. GRB 200415A, together with two other candidate giant flares (GRB 051103 and GRB 070201) follow this relation, which strongly favor the giant flare origin of these GRBs. The GeV emission detected by *Fermi*/LAT from GRB 200415A at $18 - 285\,\mathrm{s}$ can also be explained in the giant flare scenario. The total energy in the GeV emission implies a baryon load of $\sim 10^{23}$g in the giant flare fireball of GRB 200415A.

Keywords: Magnetars; Gamma-ray bursts

1. INTRODUCTION

Giant flares (GFs), with total energies in excess of 10^{44}erg, have been detected from three known SGRs. GRB 790305 is the first GF detected from SGR 0526-66 (Mazets et al. 1979; Cline et al. 1980). After $\sim$ 20 years later, two more GFs were detected, GRB 980827 from SGR 1900+14 (Hurley et al. 1999a; Feroci et al. 1999; Mazets et al. 1999b) and GRB 041227 from SGR 1806-20 (Hurley et al. 2005; Frederiks et al. 2007a). An intermediate flare (GRB 980618), with an energy of $\sim 10^{43}$ erg was detected from SGR 1627-41 (Mazets et al. 1999a; Hurley et al. 1999b). These events are now considered to be a very rare type of astrophysical phenomenon and completely different from classic short gamma-ray bursts (GRBs), which result from mergers of compact objects and occur at cosmological distance typically. On the other hand, however, if a magnetar giant flare occurs in an external galaxy, only the initial peak of a GF would be detectable, and thus the GF would resemble a several hundred millisecond long, hard-spectrum GRB (Hurley et al. 2005; Palmer et al. 2005). Indeed, two candidate giant flares have been suggested, i.e., GRB 051103, spatially coincident with the galaxy M81 (Golenetskii et al. 2005), and GRB 070201, coincident with the galaxy M31 (Mazets et al. 2008). The chance coincidence probability between the IPN localization of GRB 051103 (and GRB 070201) and a nearby galaxy is low ($\sim 1\%$; Svinkin et al. (2015)).

At 08:48:05.56 UT on 15 April 2020, the Fermi Gamma-Ray Burst Monitor (GBM) triggered and located GRB 200415A, which was also detected by *Fermi*/LAT (Bissaldi et al. 2020; Fermi GBM Team 2020; Omodei et al. 2020). Interestingly, the burst is localized by the IPN and the localization (a 274 arcmin^2 error box) shows that the Sculptor Galaxy (NGC 253) is inside the IPN box (Svinkin et al. 2020). Thus, it is possible that GRB 200415A is a GF from the Sculptor Galaxy (Svinkin et al. 2020; Frederiks et al. 2020; Pozanenko et al. 2020; Yang et al. 2020). However, without identifying the oscillatory phase or SGR activity, these candidates can not be confirmed reliably to be GFs. In this paper, we study whether the GRB 200415A is a GF and study the origin of the GeV emission.

2. GBM DATA REDUCTION AND ANALYSIS

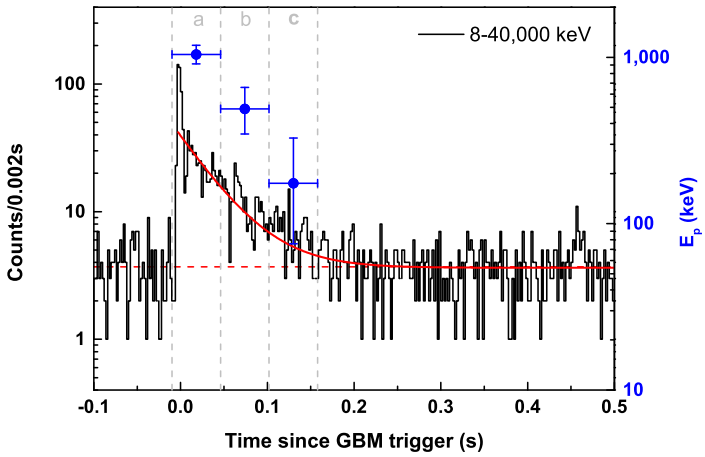

Figure 1. Light curve and E_p evolution of GRB 200415A in the GBM energy range (8–40,000 keV) on semilogarithmic scale. The red dashed line indicate the background counts. The burst decays quasi-exponentially with an e-folding time $\tau = 42.5$ ms (the red line). The gray dashed lines indicate the three intervals where the spectral peaks were measured.

GRB 200415A triggered the Fermi/GBM at 08:48:05.56 UT on 15 April 2020 (T_0) (Fermi GBM Team 2020). We select the trigger detectors, e.g., NaI detectors n0 & n1 and BGO detector b0. We first extract the time integrated spectrum in the peak region (i.e., from $T_0 - 0.010$ to $T_0 + 0.158$ s). We used the software package XSPEC (version 12.10) to perform spectral fitting. We find that the spectrum can be successfully fitted by a power law function with an exponential high-energy cutoff (hereafter, cutoff power law or CPL model), i.e., $N(E) = AE^{-\alpha}\exp[-(2-\alpha)E/E_p]$, where the $N(E)$ represents the photon number spectrum. The goodness of statistics for the fit is $PGSTAT = 327.83$ and the degree of freedom is $dof = 359$. The power law index is $-0.05^{+0.10}_{-0.10}$ and the spectral peak energy, $E_{\rm p}$, is $916.3^{+124.5}_{-112.8}$ keV. The average flux in this time interval is $(5.08 \pm 0.56) \times 10^{-5}$ erg cm^{-2} s^{-1} (between 1 keV and 10 MeV) and the total fluence is $(8.53 \pm 0.94) \times 10^{-6}$ erg cm^{-2}. Assuming that the source of GRB 200415A is situated in NGC 253 at a distance of 3.5 Mpc, the measured value of the fluence corresponds to a total isotropic energy is $E_{\rm iso} = (1.25 \pm 0.13) \times 10^{46}$ erg. We also tested the the Band function model in the spectral analysis (Band et al. 1993). We found that it also can successfully fit the spectrum, but no statistically significant high-energy power-law tail is found ($\beta < -2.95$ is not constrained well). Therefore, we favorably choose the cutoff power law model as the best-fit model in our analysis for this GRB.

The light curve of GRB 200415A observed in the GBM energy range (8–40,000 keV) with a time resolution of 2 ms is shown in Figure 1 on semilogarithmic scale. The light curve has a shape of a single short pulse ($t_{\rm burst} \sim 168$ ms) with a steep leading edge ($t_{\rm rise} \leq 6$ ms) and shows a quasi-exponential decay with an e-folding time of $\tau = 42.5$ ms. As shown in Figure 1, we divided this time interval into three segments to study its spectral evolution. We found that the spectrum displayed a strong hard-to-soft spectral evolution, which is consistent with the spectral characteristics of both GFs and classic GRBs (Hurley et al. 2005; Preece et al. 1998).

3. THE $E_{\rm P}$-$E_{\rm ISO}$ CORRELATION FOR MAGNETAR GIANT FLARES

3.1. *The GF sample*

GRB 790305 is a GF detected from SGR 0526-66 (Mazets et al. 1979). Its spectrum can be fitted by an optically thin thermal bremsstrahlung (OTTB) model $dN(E)/dE \propto E^{-1}\exp(-E/kT)$, with $kT = 520 \pm 100$ keV (Mazets & Golenetskii 1981; Mazets et al. 1982; Fenimore et al. 1996)). For this spectrum, the peak of the $E^2dN(E)/dE$ spectrum is at $E_{\rm p} = kT$. GRB 980827 is a GF detected from SGR 1900+14 (Hurley et al. 1999a). Its spectrum is also well represented by an OTTB model, so we take the peak energy $E_{\rm p}$ (averaged over a 1-s interval) as $kT = 240 \pm 20$ keV (the error bar is obtained from Figure 1 (panel b) of Hurley et al. (1999a)). GRB 041227 is a GF detected from SGR 1806-20 (Hurley et al. 2005; Palmer et al. 2005; Frederiks et al. 2007a). The spike's intensity drove all X- and γ-ray detectors into saturation, but particle

Table 1. Properties of magnetar GFs and Candidates

GRB	SGR or associated galaxy	D_L kpc	$E_{\rm iso}$ erg	$E_{\rm p}$ keV
790305[a]	SGR 0526–66 (LMC)	49.97 ± 0.19	$(6.99 \pm 0.05) \times 10^{44}$	520.0 ± 100.0
980618[b]	SGR 1627–41	11.0 ± 0.3	$(1.08 \pm 0.06) \times 10^{43}$	125.0 ± 25.0
980827[c]	SGR 1900+14	12.5 ± 1.7	$(2.99 \pm 0.81) \times 10^{44}$	240.0 ± 20.0
041227[d]	SGR 1806–20	$8.7^{+1.8}_{-1.5}$	$(7.23^{+2.99}_{-2.49}) \times 10^{45}$	480.0 ± 40.0
051103[e]	M81	3630 ± 340	$(7.12 \pm 1.33) \times 10^{46}$	~ 900.0
070201[f]	M31	744 ± 33	$(1.36 \pm 0.12) \times 10^{45}$	$296.0^{+38.0}_{-32.0}$
200415A[g]	Sculptor Galaxy (NGC 253)	3500 ± 200	$(1.25 \pm 0.14) \times 10^{46}$	$916.3^{+124.5}_{-112.8}$

[a] Pietrzyński et al. (2013); Mazets et al. (1982, 2008)

[b] Corbel et al. (1999); Mazets et al. (1999a)

[c] Davies et al. (2009); Hurley et al. (1999a); Tanaka et al. (2007)

[d] Bibby et al. (2008); Palmer et al. (2005)

[e] Freedman et al. (1994); Frederiks et al. (2007b); Mazets et al. (2008)

[f] Vilardell et al. (2010); Mazets et al. (2008)

[g] Rekola et al. (2005) and this work.

detectors aboard RHESSI and Wind made reliable measurements (Hurley et al. 2005). The SOPA and ESP instruments located on geosynchronous satellites also measured the flux and spectrum(Palmer et al. 2005). The SOPA data of this GF were fitted with a CPL model, and we take the spectral peak energy and flux from Palmer et al. (2005). GRB 980618 is an intermediate flare detected from SGR 1627-41 and its spectrum can be modelled by an OTTB spectrum (Mazets et al. 1999a). From Figure 3 of Mazets et al. (1999a), we can infer that the spectral peak of the $E^2dN(E)/dE$ spectrum is equal to $kT = 100 - 150$ keV (here we set $E_{\rm p}$ to 125 ± 25 keV). The hard spectrum of this flare, together with a total energy of 10^{43} erg, makes it quite similar to giant flares. Indeed, Mazets et al. (2008) consider this flare as a giant flare. For these reasons, we include the flare from SGR 1627-41 in the correlation analysis. Two GF candidates, GRB 051103 (Frederiks et al. 2007b) and 070201 (Mazets et al. 2008) are both well fitted by the CPL model. The spectral peak energies of these two GFs are taken from Mazets et al. (2008).

The spectral peak energy and the total isotropic energy of GRB 200415A, together with those of four GFs and two GF candidates, are summarized in Table 1. Note that, in Table 1, we also give the uncertainty in the total isotropic energy of GFs due to the uncertainty in the source distance.

3.2. $E_{\rm p}$-$E_{\rm iso}$ *Correlation*

With the observed properties of these magnetar GFs and candidates, we study relation between the spectral peak energy $E_{\rm p,z}$ and the isotropic energy $E_{\rm iso}$ of them. Since the samples in this work is small, the scaling relations are estimated by ordinary least squares for an ensemble of datasets where the data point are selected by bootstrap resampling and have positions jiggled by values consistent with their uncertainties (considering both the uncertainties of $E_{\rm p}$ and $E_{\rm iso}$). The best-fit results of the slopes and intercepts are set to be the median of the distribution of the ensemble, and the uncertainties of them are calculated by 1σ confidence intervals, which is obtained from the distribution of the ensemble.

We first use the three identified GFs and the intermediate flare for the study. The best-fit relation between the peak energy $E_{\rm p}$ and the total isotropic energy $E_{\rm iso}$ is $\log(E_{\rm p}/{\rm keV}) = (2.78^{+0.06}_{-0.05}) + (0.22^{+0.04}_{-0.05}) \log(E_{\rm iso}/10^{46}{\rm erg})$, with a Pearson correlation coefficient of $\kappa = 0.91$ and a chance probability of $p = 0.09$. If we consider only the three identified GFs, the correlation becomes weaker, but the slope is consistent with the above analysis, i.e., $\log(E_{\rm p}/{\rm keV}) = (2.73^{+0.06}_{-0.05}) + (0.15^{+0.06}_{-0.05}) \log(E_{\rm iso}/10^{46}{\rm erg})$, with a Pearson correlation coefficient of $\kappa = 0.64$. As shown in Figure 2, plotting GRB 200415A onto the $E_{\rm p}$ vs. $E_{\rm iso}$ plane, we find that GRB 200415A is in good agreement with this relation and far away from the short GRB population. This indicates that GRB 200415A is more likely to be a magnetar GF from the Sculptor Galaxy.

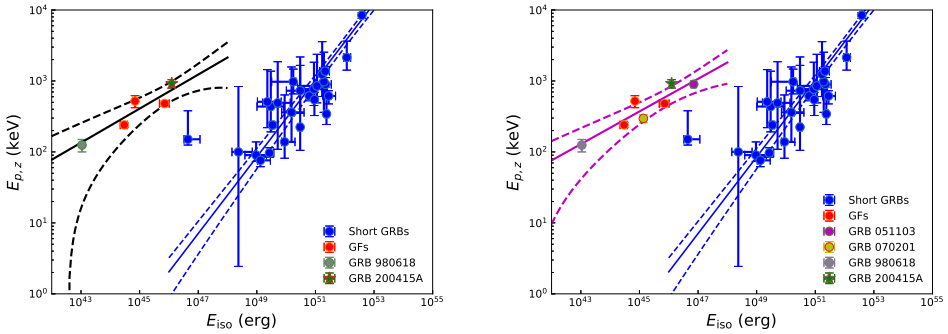

Figure 2. GRB 200415A in the $E_{\rm p,z}$-$E_{\rm iso}$ correlation diagram. The blue data points represent short GRBs, which are taken from Zhang et al. (2018). The GFs (red), intermediate flare GRB 980618 from SGR 1627-41 (green) and GF candidates (yellow and magenta) marked as the color data points are derived from the references as shown in Table 1. The green star represents GRB 200415A. The blue solid line is the best fit correlation: $\log(E_{\rm p,z}/{\rm keV}) = (3.55 \pm 0.07) + (0.54 \pm 0.04)\log(E_{\rm iso}/10^{52}{\rm erg})$ for short GRBs. The blue dashed lines represent the 1σ region of the correlation. Left panel: The black solid line represents the best-fit correlation: $\log(E_{\rm p}/{\rm keV}) = (2.85^{+0.04}_{-0.05}) + (0.24^{+0.04}_{-0.03})\log(E_{\rm iso}/10^{46}{\rm erg})$ for considering three identified GFs, the intermediate flare and GRB 200415A. The black dashed lines represent 3σ region of the correlation. Right panel: The magenta solid line is the best-fit correlation for considering three identified GFs, the intermediate flare and three candidates (including GRB 051103, 070201 and 200415A): $\log(E_{\rm p}/{\rm keV}) = (2.80^{+0.02}_{-0.03}) + (0.23^{+0.03}_{-0.02})\log(E_{\rm iso}/10^{46}{\rm erg})$. The magenta dashed lines represent 3σ regions of the correlation. The discrepant blue data point of short GRB at $E_{\rm iso} \sim 10^{46.5}$ erg represents GRB 170817A/GW 170817.

Including the three GFs, the intermediate flare, and GRB 200415A to do the re-fitting, we find that the best-fit relation gives a tighter relation: $\log(E_{\rm p}/{\rm keV}) = (2.85^{+0.04}_{-0.05}) + (0.24^{+0.04}_{-0.03})\log(E_{\rm iso}/10^{46}{\rm erg})$, with a Pearson correlation coefficient of $\kappa = 0.93$ and a chance probability of $p = 0.02$. Considering also the other two candidate GFs (GRB 051103 and GRB 070201) lying within the 3σ of the track of the GF population, we include these sources to do the re-fitting. We find that the best-fit relation gives a tighter relation: $\log(E_{\rm p}/{\rm keV}) = (2.80^{+0.02}_{-0.03}) + (0.23^{+0.03}_{-0.02})\log(E_{\rm iso}/10^{46}{\rm erg})$, with a Pearson correlation coefficient of $\kappa = 0.93$ and a chance probability of $p = 0.003$. This correlation suggests that these sources and the identified GFs are the same class of sources. This relation is quite different from the correlation for short GRBs[1], i.e., the "Amati relation" (Amati et al. 2002) with $\log(E_{\rm p,z}/{\rm keV}) = (3.55 \pm 0.07) + (0.54 \pm 0.04)\log(E_{\rm iso}/10^{52}{\rm erg})$ (Zhang et al. 2018), where $E_{\rm p,z} = E_{\rm p}(1+{\rm z})$. As shown in Figure 2, GFs do not fall on the the Amati relation of short GRBs. We also find that the two correlations do not agree at $> 5\sigma$ level, indicating that GFs are distinct from short GRBs.

3.3. *Interpretation of the scaling relation*

Next we show that the correlation between $E_{\rm p}$ and $E_{\rm iso}$ for magnetar GFs can be understood in the framework of the fireball photosphere emission model. During a GF, strong shearing of a neutron star's magnetic field, combined with growing thermal pressure, appears to have forced an opening of the field outward (Thompson & Duncan 2001). A huge amount of magnetic energy $E = 10^{46}$ erg is subsequently released at the surface of the neutron star with a radius of R_0 over a short period of $t = 0.1$ s, leading to the formation of a hot fireball (Thompson & Duncan 1995, 2001; Nakar et al. 2005), which is quite similar to the case of classic GRBs (Mészáros & Rees 2000). The optical depth for pair production is extremely high, regardless of the suppression of the effective cross-section due to the large magnetic field of the magnetar (Herold 1979). With such a large optical depth, a radiation-pairs plasma is formed at a thermal equilibrium with an initial temperature

$$kT_0 = \left(\frac{E}{4\pi R_0^2 \sigma t}\right)^{1/4} = 200\ {\rm keV} E_{46}^{1/4} R_0^{-1/2} t_{-1}^{-1/4}, \quad (1)$$

where σ is the Stephan-Boltzmann constant. This plasma expands under its own pressure, launching a relativistic outflow. As the optically thick (adiabatic) outflow expands, the comoving internal energy drops as $e' \propto V'^{-4/3} \propto n'^{4/3}$, where V' is the comoving volume and n' is the comoving baryon number density. The baryon bulk Lorentz factor increases as $\Gamma \propto R$ and the comoving temperature drops $T' \propto R^{-1}$. The $e^{\pm}$ pairs drop out of equilibrium (Paczynski 1986) at

[1] If GRB 200415A is not physically associated with the Sculptor galaxy, but is instead a chance coincidence and originates from an unrelated galaxy at a cosmological distance, then it could satisfy the $E_{p,z} - E_{iso}$ relation for a redshift of $z > 0.025$.

$T'_p = 17$ KeV at a radius of $R_p = R_0(T_0/T'_p)$. This is the radius of an $e^{\pm}$ pair photosphere. If the outflow carries enough baryons, the baryonic electrons lead to a photosphere larger than R_p. As long as the outflow remains optically thick, it is radiation dominated and continues to expand with $\Gamma \propto R$. For large baryon loads, Γ reaches the saturation value η at a radius $R_s = \eta R_0$, where the baryon load is parameterized by $\eta = E/Mc^2$. Above the saturation radius, the flow continues to coast with $\Gamma = \eta$.

On the other hand, for low baryon loads, a baryonic electron photosphere appears in the accelerating portion $\Gamma \propto R$. An electron scattering photosphere is defined by $\tau = \sigma_{\rm T} n' R_{ph}/\Gamma = 1$, where τ is the Thomson optical depth, $\sigma_{\rm T}$ is the Thomson cross-section, $n' = (L/4\pi m_p c^3 \Gamma \eta)$ is the comoving baryon density, r/Γ is a typical comoving length, m_p is the proton mass, and L is the total power of the burst. There is a critical value of η at which $R_{ph} = R_s$, i.e.,

$$\eta_* = \left(\frac{L\sigma_{\rm T}}{4\pi m_p c^3 R_0}\right)^{1/4} = 100 L_{47}^{1/4} R_{0,6}^{-1/4}. \quad (2)$$

Thus, for low baryon loads where $\eta \geq \eta_*$, the outflow becomes optically thin in the accelerating portion. The outflow emits a quasi-blackbody spectrum as it became optically thin, with a spectral temperature comparable to the temperature at its base, because declining temperature in the outflow is compensated by the relativistic blueshift, i.e., $T_{ph} = \Gamma T'_{ph} = T_0$. The observed photospheric thermal luminosity is $L_{ph} = 4\pi R^2 \Gamma^2 \sigma T'^4_{ph} = 4\pi R_0^2 \sigma T_{ph}^4$. Thus, the observer-frame photospheric temperature is

$$kT_{\rm ph} = \left(\frac{E_{\rm iso}}{4\pi R_0^2 \sigma t}\right)^{1/4} = 200 \text{ KeV} E_{\rm iso,46}^{1/4} R_0^{-1/2} t_{-1}^{-1/4}, \quad (3)$$

where $E_{\rm iso} = L_{\rm ph} t$ and we have assumed a duration of $t = 0.1$ s for the all the GFs. The peak energy of the spectrum is at $E_{\rm p} = 2.8\ kT_{\rm ph}$. It is remarkable to see that Eq.(3) agrees well with the $E_{\rm p} - E_{\rm iso}$ relation that we found for GFs.

The spectra of GRB 200415A and some other GFs are not purely blackbody and better modelled by CPL spectrum. This can be interpreted as being due to the extra contribution by some other radiation components to the low-energy spectrum, such as multi-temperature blackbody emission or synchrotron emission arising from some shocks in the relativistic outflow (Mészáros & Rees 2000). There is evidence for multi sub-pulses and fast variability in the initial spike in this and other GFs. Different sub-pulses have different temperatures, so multi-temperature blackbody is naturally expected. The fast variability implies unsteady outflow, so internal shocks could occur, which may produce a flat synchrotron spectrum. If this synchrotron spectrum is subdominant compared with the photosphere emission, the low-energy spectrum will be flatter while the peak energy remains unchanged (Mészáros & Rees 2000). A detailed study of the spectrum considering these effects is beyond the scope of the present paper.

Note that Eq.(3) holds only when $R_{ph} < R_s$, corresponding to $\eta > \eta_*$. If $R_{ph} > R_s$ ($\eta < \eta_*$), the observer-frame photospheric temperature and photospheric thermal luminosity evolve as $T_{ph} \propto R^{-2/3}$ and $L_{ph} \propto R^{-2/3}$, respectively. In this case, the relation is different from Eq.(3). That is, the temperature (or the peak energy of the spectrum) would be smaller than observed if the flow is baryon-rich, and therefore, in the present case, the outflow must be baryon-poor. This implies that baryon load in the outflow of GRB 200415A should satisfy the condition $\eta > \eta_*$.

The outflow reaches a Lorentz factor of $\Gamma = R_{ph}/R_0 = \eta_*(\eta/\eta_*)^{-1/3}$ at the photosphere. Beyond the photosphere, most of the electrons above the photosphere can still scatter with a decreasing fraction of free-streaming photons as long as the comoving Compton drag time is less than the comoving expansion time (Mészáros & Rees 2000). As a result, for $\eta > \eta_*$, the terminal Lorentz factor of the outflow is η_* (instead of η). The energy that remains in the baryons of the outflow is $E_b = E(\eta_*/\eta)$. The energy in the afterglow emission of GFs could place a limit on the energy in the final baryonic ejecta[2]. The fluence of the GeV emission of GRB 200415A is about $(2.9 \pm 0.2) \times 10^{-6}$ erg cm^2 in the time interval $0 - 300$ s, which is only a factor of 3 smaller than the fluence of the GF. This implies that η should not be much larger than η_*. As a result, we estimate that the baryon load in the GF of GRB 200415A is about $M \sim E/(\eta_* c^2) \sim 10^{23}$g.

4. ORIGIN OF THE GEV EMISSION

Remarkably, this event was detected by *Fermi*/LAT in the GeV band (Omodei et al. 2020). The *Fermi*/LAT data for the GRB 200415A was taken from the Fermi Science Support Center[3]. The data analysis was performed using the publicly available software *fermitools* (ver. 1.0.0) with the unbinned likelihood analysis method. Assuming a power-law spectrum of the burst, we estimated the best-fit *Fermi*/LAT position

[2] The kinetic energy of the outflow in the giant flare of SGR 1806-20 is constrained by the radio afterglow (Gaensler et al. 2005; Gelfand et al. 2005; Granot et al. 2006).

[3] https://fermi.gsfc.nasa.gov

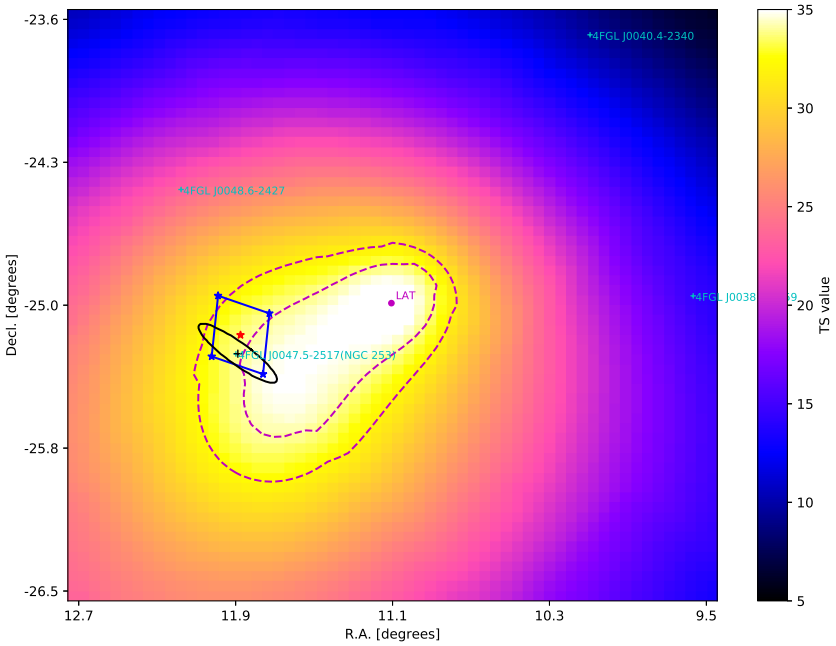

Figure 3. $3^\circ \times 3^\circ$ TS map of the GRB 200415A in the energy band 0.1-10 GeV. The green crosses represent the positions of the 4FGL point sources. Black contour depicts the optical emission from the whole NGC 253 with contour level of constant surface brightness of 25 mag arcsec^{-2} as used in Pence (1980), the black cross represents the the optical centre of the NGC 253. The magenta point indicates the best localization of GRB 200415A. The two magenta dashed circles represent the localization contours of GRB 200415A in 68% and 90% confidence levels. The red (center) and blue stars (corners) represent the IPN error box of GRB 200415A (Svinkin et al. 2020). This map has been created for a pixel size of 0.05, smoothed by gaussian kernel ($\sigma = 0.35^\circ$). The color bar represents the value of TS per pixel.

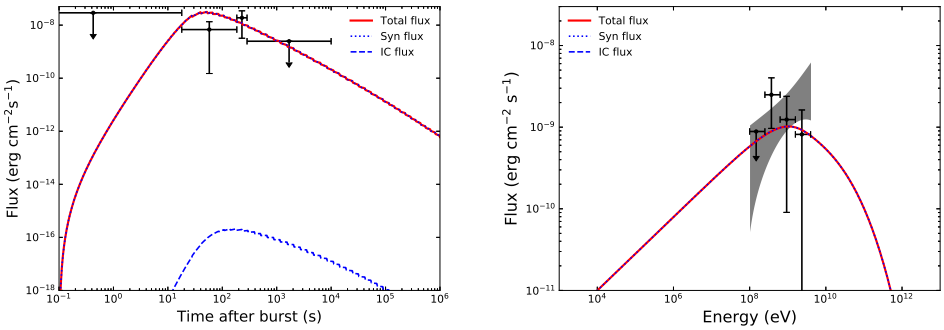

Figure 4. Left panel: modeling of the light curve of the GeV emission of GRB 200415A. The dotted curve and dashed curve represent the synchrotron component and SSC component, respectively. Right panel: modeling of the spectrum of the GeV emission of GRB 200415A at t =18–285 s. The black data points represent the GeV flux spectra of GRB 200415A. The grey butterfly shows the best fit power-law model with 1σ error. The parameters used in the fitting are $E = 1.25 \times 10^{46}$ erg, $n = 1 \times 10^{-5}$ cm^{-3}, $\epsilon_e = 0.95$, $\epsilon_B = 0.08$, $\Gamma_0 = 100$, and $p = 2.1$.

of GRB 200415A with the tool *gtfindsrc*: (11.10°, -25.03°) with circular errors of 0.41° and 0.68 ° (statistical only), respectively at 68% and 90% confidence levels. In order to reduce the contamination from the γ-ray Earth limb, the maximum zenith angle is set to be 90°. The *P8R3_TRANSIENT020_V2* set of instrument response functions is used. Since the highest-energy photon of GRB 200415A is a 1.72 GeV event, which is observed 284 seconds after the GBM trigger, we only consider the events with energies from 100 MeV to 10 GeV. Taking into the consideration of background point-like sources, Galactic diffuse and isotropic emission, we found the test statistic (TS) of the burst is 35.9 ($\sim 6\sigma$) at T_0 to $T_0 + 300$ s. The TS value is defined as $\mathrm{TS} = 2(\ln \mathcal{L}_1 - \ln \mathcal{L}_0)$, where $\mathcal{L}_0$ is the likelihood of background (null hypothesis) and $\mathcal{L}_1$ is the likelihood of the hypothesis for adding the burst. The averaged flux is $(9.52 \pm 0.61) \times 10^{-9}$ erg cm^{-2} s^{-1} with a photon index -1.46 ± 0.37.

As shown in Figure 3, we compare the localization of LAT for GRB 200415A with the IPN error box and the position of NGC 253 (4FGL J0047.5–2517). We find that the NGC 253 is located inside the IPN error box, and the error box center is offset by 5.93 arcmin from the NGC 253. The IPN error box is almost inside the region of the localization contours of GRB 200415A at the 90% confidence level. Considering also the temporal coincidence between the GeV emission and the giant flare, we suggest that the GeV emission of GRB 200415A originates from the NGC 253.

We perform modeling of the *Fermi*/LAT data for GRB 200415A using the numerical code (Liu et al. 2013). According to the standard afterglow model (Sari 1997), the light curve for a given observed frequency (ν) could be calculated as $F(t,\nu) = F(t,\nu,E_k,n,p,\varepsilon_e,\varepsilon_B,\Gamma_0)$, employing a numerical code developed in our previous work (Liu et al. 2013). E_k is the isotropic kinetic energy of the GRB outflow, n is the particle number density of the ambient medium, p is the electron spectral index, ε_e and ε_B are the equipartition factors for the energy in electrons and magnetic field in the shock, and Γ_0 is the initial Lorentz factor of the outflow.

While GeV afterglow emission is commonly seen in short GRBs, it can not be taken as evidence against the magnetar GF origin. Indeed, GRB200415A is the first GF observed by *Fermi*/LAT, which has started operation since 2008. We suggest that the GeV emission may be produced by the shocks arising from the interaction between the relativistic outflow and the ambient medium. Generally there are two shocks, one is the forward shock expanding into the ambient medium and the other is the reverse shock expanding into the outflow ejecta. Both shocks could accelerate electrons, producing synchrotron emission and inverse-Compton emission. Below we study the possibility of the forward shock emitting the GeV afterglow emission. Since the terminal Lorentz factor of the relativistic outflow after the acceleration is η_*, we take $\Gamma_0 = 100$ as a reference value for the initial Lorentz factor of the forward shock. The modeling results of the afterglow light curve and SED for GRB 200415A are shown in Figure 4. The low density of the ambient medium is not surprising, since the pulsar wind and earlier SGR activity from the magnetar may have created a cavity around the pulsar. Indeed, it has been suggested that the Poynting flux emanating from the pulsar can excavate a bow-shock cavity around the pulsar with a size as large as fractions of a parsec (Holcomb et al. 2014). Interestingly, a bow-shock environment was discussed in Granot et al. (2006) to explain the radio nebula from the afterglow of the GF from SGR 1806-20. The value of the electron equipartition factor $\epsilon_e = 0.95$ seems to be higher than that inferred for classic GRBs, but considering that the ambient medium around the pulsar may be enriched with pairs, such a value of ϵ_e may be reasonable for magnetar GFs (Konigl & Granot 2002). We would like to point out that the model parameters cannot be reliably determined and the set of parameters we quoted is only an illustrative example.

5. CONCLUSIONS

Magnetar giant flares, if occurring in nearby galaxies, would appear as cosmic short-hard GRBs. Thus, identifying the nature of such kind of short GRBs becomes a challenge. In this paper, we have shown that magnetar giant flares locate in a distinct region of the $E_{\rm p} - E_{\rm iso}$ plane and follow a scaling relation roughly as $E_{\rm p} \propto E_{\rm iso}^{1/4}$, quite different from those of classic short GRBs. Although the number of giant flares in our sample is small, the scaling relation is well consistent with the expectation of the standard model of magnetar giant flares, which ascribes the formation of the hot fireballs as a consequence of catastrophic instabilities in magnetars (Thompson & Duncan 2001). Such a scaling relation thus provides a powerful tool to distinguish between magnetar giant flares and classic short GRBs. Along this line, we suggest that GRB 200415A is a magnetar giant flare occurred in the nearby galaxy NGC 253.

ACKNOWLEDGMENTS

We thank the referee for the constructive report. The work is supported by the NSFC grants 11625312 and

11851304, and the National Key R & D program of China under the grant 2018YFA0404203.

REFERENCES

Amati, L., Frontera, F., Tavani, M., et al. 2002, A&A, 390, 81

Band, D., Matteson, J., Ford, L., et al. 1993, ApJ, 413, 281

Bibby, J. L., Crowther, P. A., Furness, J. P., et al. 2008, MNRAS, 386, L23

Bissaldi, E., Briggs, M., Burns, E., et al. 2020, GRB Coordinates Network, Circular Service, No. 27587, 27587

Cline, T. L., Desai, U. D., Pizzichini, G., et al. 1980, ApJL, 237, L1

Corbel, S., Chapuis, C., Dame, T. M., et al. 1999, ApJL, 526, L29

Davies, B., Figer, D. F., Kudritzki, R.-P., et al. 2009, ApJ, 707, 844

Duncan, R. C. & Thompson, C. 1992, ApJL, 392, L9

Fenimore, E. E., Klebesadel, R. W., & Laros, J. G. 1996, ApJ, 460, 964

Fermi GBM Team 2020, GRB Coordinates Network, Circular Service, No. 27579, 27579

Feroci, M., Frontera, F., Costa, E., et al. 1999, ApJL, 515, L9

Freedman, W. L., Hughes, S. M., Madore, B. F., et al. 1994, ApJ, 427, 628

Frederiks, D. D., Golenetskii, S. V., Palshin, V. D., et al. 2007a, Astronomy Letters, 33, 1

Frederiks, D. D., Palshin, V. D., Aptekar, R. L., et al. 2007b, Astronomy Letters, 33, 19

Frederiks, D., Golenetskii, S., Aptekar, R., et al. 2020, GRB Coordinates Network, Circular Service, No. 27596, 27596

Gaensler, B. M., Kouveliotou, C., Gelfand, J. D., et al. 2005, Nature, 434, 1104

Gelfand, J. D., Lyubarsky, Y. E., Eichler, D., et al. 2005, ApJL, 634, L89

Granot, J., Ramirez-Ruiz, E., Taylor, G. B., et al. 2006, ApJ, 638, 391

Golenetskii, S., Aptekar, R., Mazets, E., et al. 2005, GRB Coordinates Network, Circular Service, No. 4197, #1 (2005), 4197

Herold, H. 1979, PhRvD, 19, 2868

Holcomb, C., Ramirez-Ruiz, E., De Colle, F., et al. 2014, ApJL, 790, L3

Hurley, K., Cline, T., Mazets, E., et al. 1999a, Nature, 397, 41

Hurley, K., Kouveliotou, C., Woods, P., et al. 1999b, ApJL, 519, L143

Hurley, K., Boggs, S. E., Smith, D. M., et al. 2005, Nature, 434, 1098

Königl, A. & Granot, J., 2002, 574,134

Lipunov, V., Tyurina, N., Gorbovskoy, E., et al. 2020, GRB Coordinates Network, Circular Service, No. 27599, 27599

Liu, R.-Y., Wang, X.-Y., & Wu, X.-F. 2013, ApJL, 773, L20

Mazets, E. P., Golentskii, S. V., Ilinskii, V. N., et al. 1979, Nature, 282, 587

Mazets, E. P. & Golenetskii, S. V. 1981, Ap&SS, 75, 47

Mazets, E. P., Golenetskii, S. V., Gurian, I. A., et al. 1982, Ap&SS, 84, 173

Mazets, E. P., Aptekar, R. L., Butterworth, P. S., et al. 1999a, ApJL, 519, L151

Mazets, E. P., Cline, T. L., Aptekar', R. L., et al. 1999b, Astronomy Letters, 25, 635

Mazets, E. P., Aptekar, R. L., Cline, T. L., et al. 2008, ApJ, 680, 545

Mészáros, P. & Rees, M. J. 2000, ApJ, 530, 292

Nakar, E., Piran, T., & Sari, R. 2005, ApJ, 635, 516

Omodei, N., Axelsson, M., Piron, F., et al. 2020, GRB Coordinates Network, Circular Service, No. 27586, 27586

Paczynski, B. 1986, ApJL, 308, L43

Palmer, D. M., Barthelmy, S., Gehrels, N., et al. 2005, Nature, 434, 1107

Pence, W. D. 1980, ApJ, 239, 54

Pietrzyński, G., Graczyk, D., Gieren, W., et al. 2013, Nature, 495, 76

Pozanenko, A., Minaev, P., Chelovekov, I., et al. 2020, GRB Coordinates Network, Circular Service, No. 27627, 27627

Preece, R. D., Pendleton, G. N.; Briggs, M. S.; et al., ApJ, 496, 849

Rekola, R., Richer, M. G., McCall, M. L., et al. 2005, MNRAS, 361, 330

Sari, R. 1997, ApJL, 489, L37

Svinkin, D. S., Hurley, K., Aptekar, R. L., et al. 2015, MNRAS, 447, 1028

Svinkin, D., Golenetskii, S., Aptekar, R., et al. 2020, GRB Coordinates Network, Circular Service, No. 27595, 27595

Tanaka, Y. T., Terasawa, T., Kawai, N., et al. 2007, ApJL, 665, L55

Thompson, C. & Duncan, R. C. 1995, MNRAS, 275, 255

Thompson, C. & Duncan, R. C. 2001, ApJ, 561, 980

Vilardell, F., Ribas, I., Jordi, C., et al. 2010, A&A, 509, A70

Yang, J., Chand, V., Zhang, B.-B., et al., 2020, ApJ, 899, 106.

Zhang, B.-B., Zhang, B., Sun, H., et al. 2018, Nature Communications, 9, 447